# STRONG VARIABILITY IN THE DECAMETER-SCALE GEOMETRIES OF LAVA FLOW MARGINS

E. I. Schaefer[1,2], C. D. Neish[1,2], and C. W. Hamilton[3] [1]Department of Earth Sciences, Western University, London, ON N6A 5B7 Canada (ethan.i.schaefer@gmail.com), [2]The Institute for Earth and Space Exploration, Western University, London, ON N6A 5B7 Canada. [3]Lunar and Planetary Laboratory, University of Arizona, Tucson, AZ 85721 USA.

**Introduction:** The geometry of a lava flow's margin may encode important constraints on the rheology and dynamics of the flow at the time of its emplacement [1]. If so, decoding this signal on planetary surfaces would help us to understand the eruptive history and thermal evolution of the body.

Classical work [1] demonstrated that flows of morphologic types ‘a‘ā and pāhoehoe—which form under different rheological and dynamical conditions [2–4]—can be distinguished by fractal analysis of their margins, which measures geometric roughness [5]. More recently, we have shown that this fractality can be (1) markedly scale-dependent and (2) substantially modified by topography and sedimentation [6,7]. Moreover, we showed that so-called transitional flow types, which may be common on planetary surfaces [8–10] and have debated formation conditions [11], can have meter-scale margin geometries similar to those of ‘a‘ā and pahoehoe flows, resulting in interpretive ambiguity [6] at meter scales.

Here, we focus on margin geometries at coarser scales (>10 m), which have some promising attributes for remotely interpreting planetary lava flows:

- more broadly resolved in planetary data sets
- less likely to be modified by unresolved topography or modest sedimentation or erosion
- potentially represent a different regime than the ambiguous meter-scale geometries [6,12] but still reflect emplacement conditions [1,13].

**Study Site and Methods:** Our study site is the 2014–2015 Holuhraun flow field, Iceland. Numerous studies and abundant data provide key constraints on the effusion rates [14–16], structure and evolution [17], and morphologic types [17, 18] of this flow field.

For the main analysis, we use a series of Sentinel 1 radar images spaced at a mean of ~5 days, from 36 days into the eruption (Oct. 6, 2014) through the end of the eruption (Feb. 27, 2015). Unlike visible images, radar images are not obscured by the darkness of the Arctic winter, volcanic plumes, or clouds. We have rigorously aligned the images using feature detection [19] and pixel correlation [20] techniques. We are now mapping the flow margins in each consecutive image, and we restrict our analyses to time intervals where the margin advances locally both before and after the analysis interval, to reduce the risk of underestimating the true advance rate when the advance likely spans only a portion of an inter-image interval.

To estimate *local discharge* (e.g., at the scale of a lobe), we divide the areal advance by the elapsed inter-image time [cf. 15]. To estimate the *local volumetric flux*, we divide this discharge by the approximate flow front width. We measure the roughness of each margin by calculating the scale-dependent fractal dimension $D$ using the technique of [6] but restrict the minimum considered scale (rod length) to 20 m, in view of the 10-m pixel scale of the images.

**Results: Fig. 1a** shows the margins mapped so far. **Fig. 1b** and **Table 1** present results for those margins suitable for analysis (primarily determined by length).

**Discussion:** *Variability of coarse margin geometries.* Our results so far show that the mapped progressive margins can have markedly different fractalities at coarse (>10 m) scales, spanning a $D$ range of 1.04–1.20. Notably:

- This observed variability—for a single eruption—is comparable to the combined variability measured by [1] among 44 ‘a‘ā and pāhoehoe margins in a global dataset (1.05–1.23).
- Moreover, the variability at a single scale, 80 m, exceeds the scale-dependent variability we earlier measured across 0.3– 247 m for the nearby final (post-eruption) margin [6].
- Conversely, at finer scales, we earlier measured largely similar fractality everywhere along the nearby final margin [12].

To explore this last point, we took subsets of field-collected vertices along the final margin [6] to roughly parallel the Dec24b and Dec29a margins (**Fig. 1a**). Although our analysis of these subsets approximately reproduces the $D$ values of their mapped counterparts at ~80 m, $D$ values up to 4 m are nearly identical for both subsets (**Fig. 1b**). Thus, distinct geometric regimes appear to dominate fine versus coarse scales.

*What could account for this variability?* Although different morphologic types are associated with margins of different $D$ values [1,6], all analyzed margins are from flows of the same type, spiny pāhoehoe [18]. We therefore preliminarily consider four alternative causes for this variability: local discharge, local volumetric flux, general effusion rate (for the whole flow field), and flow field maturity.

As local discharge decreases from Dec12b to Dec24b to Dec17a, margin $D$ increases (**Table 1**).

However, Dec29a has intermediate discharge and the highest margin *D*.

Alternatively, we could treat Dec12b and Dec17a as one set, for which the margin advances broadly along a curvilinear front, and Dec24b and Dec29a as a second set, for which the margin advances as a discrete lobe [cf. 21]. In that speculative framing, decreasing local volumetric flux correlates with increasing margin *D* within each set, but not between sets (**Table 1**).

Estimates of the (time-varying) general effusion rate for this eruption depend on the data and technique used [14–16]. Nonetheless, measurements of the average general effusion rate (over some time interval) do not vary markedly for the last three weeks of December. Therefore, the general effusion rate appears unlikely to drive variation in margin *D,* unless the salient timescale is not resolved by these estimates.

Note that a negative correlation between margin *D* and local discharge, local volumetric flux, or general effusion rate would be broadly consistent with the observation that margins of ‘a‘ā, associated with relatively high local volumetric flux [2–4] and general effusion rates [22], have lower *D* values at coarse scales than margins of pāhoehoe [1,13].

Finally, [23] noted that for flow fields of molten wax, margin *D* tended to increase until reaching a steady state. Among the four margins analyzed so far, *D* does not show such a convergent trend (**Table 1**), though even the results of [23] had significant noise.

**Conclusions:**

1. Lava flow margin geometries appear to have distinct fine (<10 m) and coarse (>10 m) regimes.
2. At the 2014–2015 Holuhraun flow field, Iceland, coarse margin geometries exhibit strong variability that is absent at fine scales.
3. Preliminary results hint that local discharge or volumetric flux may contribute to coarse margin geometries.

**Acknowledgments:** This work is supported by the Canadian Space Agency.

**References:** [1] Bruno B. C. et al. (1994) *Bull. Volc., 56*, 193–206. [2] MacDonald G. A. (1953) *Am. J. Sci., 251*, 169–191. [3] Peterson D. W. and Tilling R. I. (1980) *J. Volc. Geoth. Res., 7,* 271–293. [4] Cashman K. V. et al. (1999) *Bull. Volc., 61*, 306–323. [5] Gneiting T. and Schlather M. (2004) *Soc. Ind. App. Math., 46*, 269–282. [6] Schaefer E. I. et al. (in review) *JGR: Solid Earth* [preprint: https://doi.org/10.1002/essoar10504418.1]. [7] Schaefer E. I. et al. (2020) *LPSC 51*, #2457. [8] Keszthelyi L. et al. (2000) *JGR: Planets, 105*, 15027–15049. [9] Keszthelyi L. et al. (2004) *Geochem., Geophys., Geosys., 5*, Q11014. [10] Voigt J. R. C. and Hamilton C. W. (2018) *Icarus*, *309*, 389–410. [11] Hamilton C. W. (2019) in: Six N. F. and Karr G. *MSFC Faculty Fellow. Prgm.*, *TM—2019–220139*, 47–56. [12] Schaefer E. I. (2019), Ph.D. thesis, U. of Arizona. [13] Bruno B. C. and Taylor G. J. (1995) *GRL, 22*, 1897–1900. [14] Coppola D. et al. (2017) *Geology, 45*, 523–526. [15] Bonny E. et al. (2018) *JGR: Solid Earth, 123*, 5412–5426. [16] Coppola D. et al. (2019) *Ann. Geophys., 62*, VO221. [17] Pedersen et al. (2017) *J. Volc. Geoth. Res., 340*, 155–169. [18] Voigt et al. (2018) *AGU*, P31H-3796. [19] Rublee E. et al. (2011) *Intl. Conf. Comp. Vision*, 2564–2571. [20] Evangelidis G. D. and Psarakis E. Z. (2008) *IEEE Trans. Patt. Anal. Mach. Intel., 30*, 1858–1865. [21] Anderson S. W. et al. (2005) *GSA Spec. Paper 396*, 147–161. [22] Rowland S. K. and Walker G. P. (1990) *Bull. Volc., 52*, 615–628. [23] Blake S. and Bruno B. C. (2000) *EPSL, 184*, 181–197.

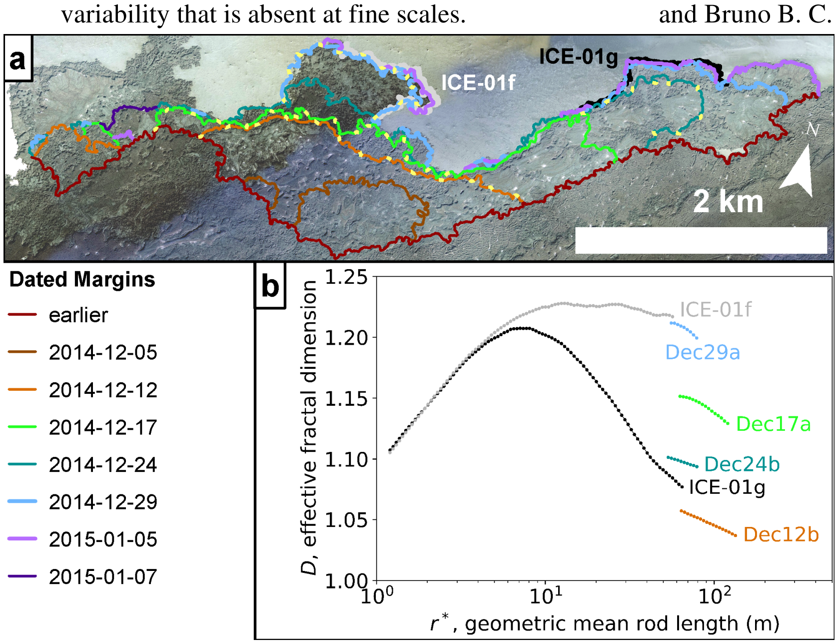


**Fig. 1**. (a) Dated margins mapped from Sentinel 1 radar images (colors) and subsets of field-collected vertices from the post-eruption margin (gray and black). For dated margins, analyzed intervals are dotted yellow and span the longest continuous interval of each margin. (b) Scale-dependent fractal analysis. Colors are the same as in (a).

**Table 1**

| Name | *D* ($r^*$ = 80 m) | Discharge ($km^2$/d) | Flux (km/d) |
|---|---|---|---|
| **Dec12b** | 1.05 | 0.132 | 0.050 |
| **Dec17a** | 1.15 | 0.031 | 0.013 |
| **Dec24b** | 1.09 | 0.053 | 0.113 |
| **Dec29a** | 1.20 | 0.065 | 0.089 |